Scanning Force Microscopy of Polyester: Surface Structure and Adhesive Properties

Ben D Beake, Nicholas J Brewer and Graham J Leggett*

Department of Chemistry, University of Manchester Institute of Science and Technology, PO Box 88, Manchester M60 1QD, United Kingdom

SUMMARY: Scanning force microscopy has been used to characterize the surface structure and properties of poly(ethylene terephthalate) (PET) films. Two types of biaxially oriented film have been studied: one (Melinex O) is free of additives while the other (Mylar D) contains particulate additives at the surface. Contact mode characterization of both materials provide clear images of the polymer surface and (in the case of Mylar D) the additives. Phase images reveal substantial nanoscale morphological detail, including small features thought to be crystallites. To model the adhesive properties of polymer surfaces, mixed self-assembled monolayers containing polar and methyl terminated adsorbates were studied using chemical force microscopy. It was found that the strength of the tip-sample adhesion increased with the fraction of polar terminated adsorbates at the surface when a carboxylic acid terminated tip was employed, while the trend was reversed when a methyl terminated tip was used. Adhesion forces measured for plasma treated PET increased with treatment time, and linearly with the cosine of the water contact angle, illustrating the chemical selectivity of chemical force microscopy. However, friction forces were found to vary in a non-linear fashion, indicating that changes to the polymer surface mechanical properties following treatment were important.

Introduction

The advent of scanning force microscopy (SFM) has facilitated considerable advances in our ability to characterize polymer surface topography[1,2]. High-resolution images of polymer surfaces are now routine. More importantly, however, SFM has provided a range of new tools with which to explore polymer surface properties quantitatively with nanometre spatial resolution. Modulation techniques, such as force modulation microscopy (FMM) and phase imaging, provide the means to probe heterogeneity in mechanical responses[3,4] and adhesive interactions; lateral force microscopy (LFM), or friction force microscopy (FFM), provides information on tip-sample frictional interactions[5,6]; and chemical force microscopy (CFM)[7] provides quantitative information on adhesive interactions. These methods offer great potential for polymer surface characterization. However, much published work to date has focused on well-defined homogeneous systems. Often, and particularly following surface

 CCC 1022-1360/00/$ 17.50+.50/0

treatment, polymers have complex, heterogeneous surfaces. We have been investigating the surface structures and properties of a variety of polyester film materials using SFM. These materials are heterogeneous in a number of senses: first, because they typically contain particulate additives; second because they have a rich nanoscale phase structure that has been the subject of intensive investigation but still presents significant problems; and third because the materials are often treated (chemically or by discharge treatment) to modify their adhesive and other properties, introducing further heterogeneities, both chemical and mechanical. Characterization of these challenging samples by conventional methodologies has been in many ways successful, but there are important novel insights that SFM methodologies are capable of providing, particularly relating to the mechanical and adhesive properties of the film surface, that are not currently available through other methods.

The objectives of the present work are first, to compare the different methods available for characterization of the untreated polymer by SFM; and second, to study the effects of surface treatment (in particular, plasma treatment). Findings are reported from studies of two types of polyester film material: Mylar D, which contains silicate particulate additives, and Melinex O, which is additive free.

Experimental

Mylar D (Du Pont) was obtained from Goodfellow Advanced Materials (Cambridge, UK) as a free-standing film and was used without further treatment. Melinex O (ICI, Wilton, UK) was supplied as a free-standing film, and was again used as received. Both materials are 100 μm thick. Self-assembled monolayers (SAMs) were prepared according to well-established procedures[8] by immersing freshly evaporated gold films, deposited onto chromium-primed glass slides, into 1 mMol solutions of thiols for approximately 18 h. Tips were coated for use in CFM experiments in exactly the same fashion. The resulting materials were extensively characterized by a variety of techniques, including static secondary ion mass spectrometry[9]. Mixed monolayers were prepared from solutions containing mixtures of dodecanethiol (DDT) and mercaptoundecanol (MUL)[8]. Immediately prior to use, the SAMs were removed from the thiol solutions, rinsed with ethanol and dried under a stream of nitrogen. Exposure to air prior to transfer to ethanol for SFM characterization was minimized (kept to less than one hour) in order to avoid ambient oxidation. Argon plasma treatment was performed using an

inductively coupled tubular reactor. An argon pressure of 0.1 mbar and a discharge power (forward – reverse) of 10 W were employed.

SFM was performed on a Digital Instruments Nanoscope IIIa multimode atomic force microscope. Contact mode imaging was performed using a range of silicon nitride cantilevers (Digital Instruments Nanoprobes, nominal force constants 0.06 – 0.58 $N \cdot m^{-1}$). The force constants of these cantilevers were determined from measurements of their resonant frequencies by a method implemented by the instrument software, based on a method developed by Cleveland *et al*[10]. Such measurements are subject to an *absolute* uncertainty of approximately 30%. However, variation in force constants for cantilevers taken from a specific wafer was relatively small (all of the cantilevers used for force-distance measurement and FFM in the present study were taken from a single wafer of Nanoprobes) meaning that the *relative* comparability of different results taken on our instrument alone is substantially better. Therefore, results of force-distance measurements are quoted as forces (in nN), although the purpose of the data presented in Fig.s 5, 7 and 8 is to show relative changes in adhesion forces for samples in a specific series. The error bars shown do not include an estimation of the absolute uncertainty, but instead show the standard error in the mean of measurements taken with a specific cantilever. Each data point represents the mean of approximately 100 measurements (typically 10 at each of 10 different locations). A different cantilever was employed for each of Fig.s 5, 7 and 8, so absolute forces may not readily be compared between figures, although trends and the magnitudes of relative changes may be accurately compared.

The treatment of friction force measurements is even more problematic, because of the greater difficulty in determining torsional spring constants by experimental methods[11]. While there are, alternatively, methods that involve calculations based on cantilever dimensions and properties[12], or finite element analysis[13], these are not straightforward to apply. In the present study, we have chosen to use relative values of friction forces, rather than attempting to determine absolute ones. Where friction "forces" are shown they are effectively obtained in units of photodetector voltage, by subtraction of forward and reverse direction scans along a single line, recorded in the scope mode of the microscope at ten separate points on the sample surface and averaged, with a fixed scan velocity. The error bars are equal to the standard deviation. Friction coefficients μ were determined from the gradient of a plot of the friction

"force" F against the applied load L over a range of loads from 0 to 80 nN. In this range, the data were found to exhibit a linear relationship, in accordance with Amonton's law[14]:

$$F = \mu L.$$

In view of the uncertainty in the absolute value of the friction "force", it was necessary to measure μ for each sample in a particular series using a single cantilever. This approach has been adopted by other authors (for example, see the work of Lee *et al*[15]). While it means that absolute values for μ may not directly be compared with those determined on other instruments, comparison of the measurements for samples in a specific series is still significant. Such relative changes reveal important differences in the behavior of the materials studied here. After completion of a set of measurements, selected values were determined a second time and compared with the original measurements, to ensure that deterioration of the sample or the cantilever had not occurred (which would lead to a change in the measured value of μ).

Height and phase shift images of the film surfaces were acquired in Tapping Mode using "Nanosensors", silicon cantilevers with resonant frequencies of *ca.* 280-300 kHz obtained in wafer form from LOT Oriel, (Leatherhead, UK). According to the specifications, the probes had typical tip radii of 10 nm and a cone half angle of 18° front to back. Tapping was performed in air at the resonant frequency of the cantilever. The level of the tip-sample interaction force was controlled by adjustment of two parameters: the amplitude of the free oscillation of the cantilever, A_0, and the ratio of the amplitude of set-point oscillation to this free oscillation, r_{sp}. A_0 was typically 22-36 nm. Exact values are given in the figure captions. Scan rates were in the range 0.5-2 Hz.

Results and Discussion

Characterization of Untreated Polyester Film

Fig. 1 shows a 10 μm × 10 μm contact mode image of the surface of Mylar D. The additive particles are clearly resolved. They are relatively uniformly distributed at the surface, although there is some variation in size. Radial features may be observed centered on some of the larger additive particles. These have previously been tentatively ascribed to strain-induced crystallization[16]. Images of Melinex O were, by comparison, quite featureless. The surface roughness was remarkably low, with the z-scale extending only as far as 15 nm in an area as

large as 9 μm^2. FFM images of Melinex O were featureless, in accordance with the expected homogeneity of the surface. However, FFM images of Mylar D exhibited clear differences in the behavior of polymer and additive materials, with the hard silicate additives exhibiting low friction (dark contrast) compared to the surrounding polymeric material (Fig. 2).

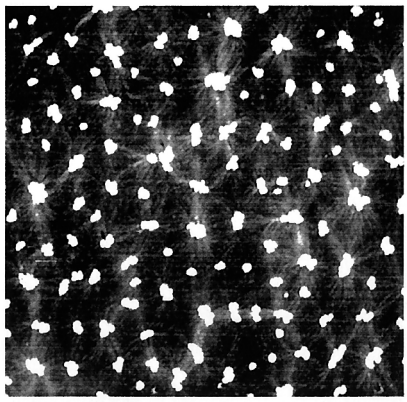

Fig. 1. Contact mode images of Mylar D. Image size: 10 μm × 10 μm. The z-scale spans 0 – 10 nm.

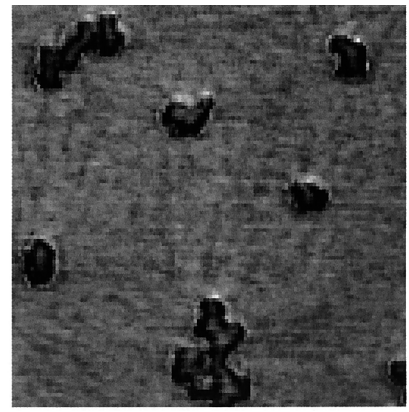

Fig. 2. Friction force microscopy image of Mylar D. Image size: 2 × 2 μm. z-scale 0 – 0.2 V.

For both polymers, the tapping mode topographical images were very similar to those recorded in contact mode. Under conditions other than those of very "light tapping", however, the phase images revealed greater detail. With r_{sp} set close to unity (light tapping), it has been suggested that the tapping force is low and the probe response is dominated by capillary and adhesive interactions[17]. Under these conditions, the silicate additives exhibited bright contrast compared to the surrounding polymer, but comparatively little detail was observed (images not shown). Other workers have reported reduced image quality under these conditions. However, on decreasing r_{sp} to values in the range 0.4 – 0.6 ("moderate tapping"[18,19]), a large phase shift was observed between the silicate additives and the polymer background, with the silicates exhibiting contrast that is brighter (by 30 – 40°) than the surrounding polymer (Fig. 3). A wealth of detail was observed in phase images recorded under these conditions that was not present in the contact mode images. The additive particles were seen to have irregular shapes (Fig. 3), and much detailed structure was observed. Importantly, the surface of the polyester also exhibited a great deal of detail, and appeared to be covered with small features of the order of a few nm in width and up to a few tens of nm in length. These features exhibited bright contrast. Increasing the imaging force, by decreasing r_{sp}, is thought to result

in contrast becoming dominated by the mechanical properties of the sample[19]. In Fig. 3 it may thus be reasonable to attribute the contrast variations to differences in sample stiffness, implying that the bright features in Fig. 3 are stiffer than the surrounding polymeric material.

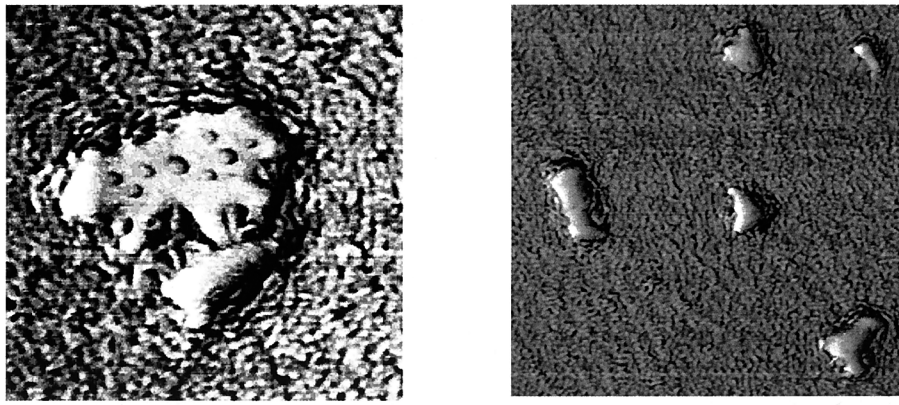

Fig. 3. Phase images of Mylar D. Left: 0.6 μm × 0.6 μm, contrast 0 – 15°, A_0 = 25 nm, r_{sp} = 0.40. Right: 1.34 × 1.34 μm, contrast 0 – 20°, A_0 = 26 nm, r_{sp} = 0.43.

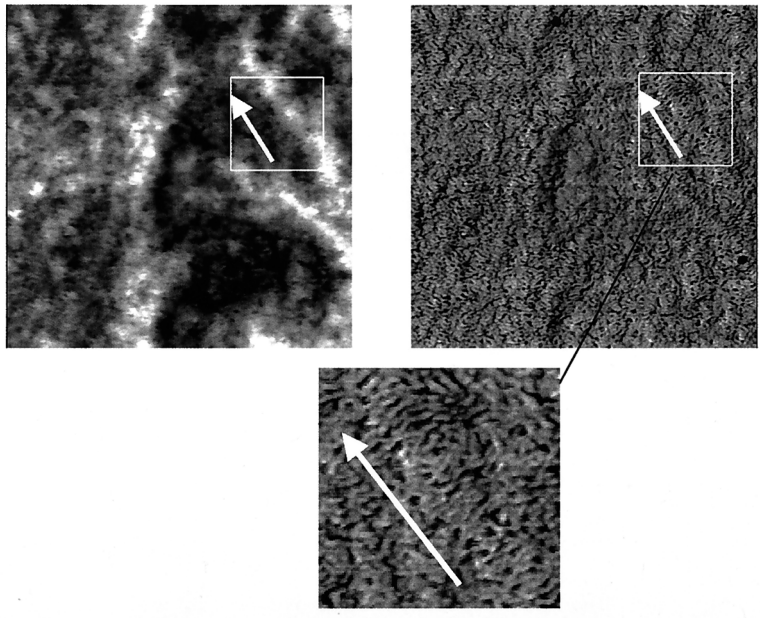

Fig. 4. Tapping mode topographical image (left) and phase images (right and bottom) of Melinex O. Main images 1.5 μm × 1.5 μm.

Similar features were observed in images of Melinex O (Fig. 4). Careful examination of the tapping mode (topographical) image on the left of Fig. 4 reveals several raised features, resembling fibrils, running across the imaged area. When these features were compared in the phase image, bright features, like those observed all over the surface of the material, were observed but oriented with their long faces aligned predominantly perpendicular to the director of the raised feature (see zoomed image). The similarity in the morphologies observed for these two materials suggests that they are generally characteristic of biaxially oriented polyester films, rather than being artifacts of differing manufacturing processes. There has been much discussion of the crystal structure of biaxially oriented polyester films such as Mylar and Melinex. Detailed studies by such techniques as small-angle X-ray scattering have indicated that the crystallites are small plate-like structures – probably having dimensions on the order of nm – and are quite unlike the larger spherulitic crystals often characteristic of thermoplastics[20,21]. Previously there has been no direct visualization of the crystallites in PET films. It is possible that the features observed in Fig.s 3 and 4 are crystallites, viewed edge-on. Under the conditions used in the present study, the brighter contrast they exhibit in the phase images is consistent with this identification. Their dimensions are close to those determined for PET crystallites by other methods, and their density at the surface is high, consistent with the known high crystallinity of Mylar D and Melinex O[20,21].

Model Heterogeneous Systems

We wished to investigate the extent to which scanning force microscopy could elucidate the nature of the changes at the polymer surface occurring following plasma treatment. In order to obtain a better understanding of the nanoscale adhesive properties of the treated polymer, we planned to use FFM in combination with CFM, in which a SAM is deposited onto an SFM tip to give it a specific chemical functionality[7]. Plasma treated polymers represent extremely challenging subjects for investigation by CFM. To date, with few exceptions[22,23,24], the majority of published studies have focused on well-defined systems – principally self-assembled monolayers. In order to examine the sensitivity of these methods for such complex systems, we first performed measurements on model heterogeneous systems. Mixed self-assembled monolayers (SAMs), formed by the coadsorption of methyl terminated thiols with either hydroxyl or carboxylic acid terminated thiols, were used to create surfaces with

chemical heterogeneity. These materials have been extensively studied by other groups, including, in particular, Whitesides and co-workers[25]. By adsorbing monolayers from solutions containing thiols with contrasting terminal group chemistries, it was possible to prepare surfaces with a range of compositions, ranging from non-polar to polar.

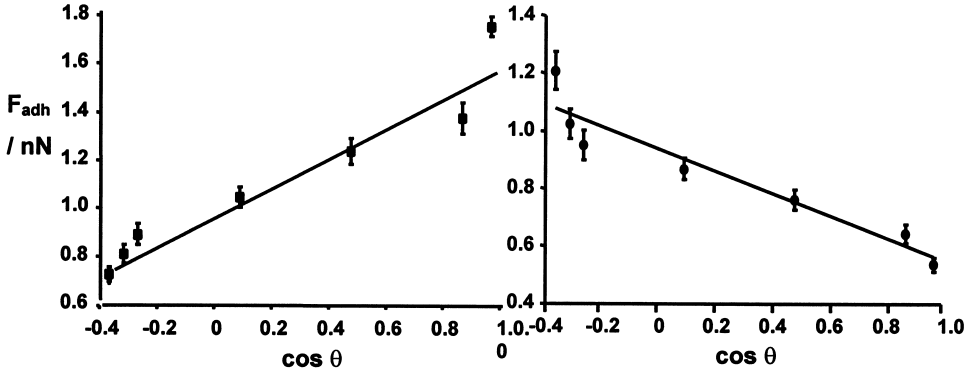

Fig. 5. Left: variation in the adhesion force measured using an acid terminated tip with the water contact angle for mixed SAMs containing methyl and hydroxyl terminated thiols. Right: variation in the adhesion force measured when a methyl terminated tip is used.

Because it was known from contact angle measurements that plasma treatment led to the incorporation of polar groups at the PET surface, adhesion force measurements were initially carried out with polar tips. Fig. 5 shows adhesion force measurements carried out for a series of mixed methyl/hydroxyl terminated SAMs using a carboxylic acid terminated tip, derivatized with a monolayer of mercaptoundecanoic acid. The pull-off force is plotted against the cosine of the water contact angle for each system. Cosθ gives a measure of the fraction of polar terminated molecules in the SAM, and is also related to the surface free energy by Young's equation:

$$\gamma_{LV}\cos\theta = (\gamma_{SV} - \gamma_{SL})$$

It may be seen that the adhesion force increases from low values for $\cos\theta = 0$ to higher values at $\cos\theta = 1$, and that the magnitude of the overall change is significant compared to the uncertainty in the mean value at each composition.

Use of a carboxylic acid terminated tip should mean selectivity for polar interactions; the increasing adhesion force as the fraction of polar groups in the monolayer increases reflects the fact that the polar groups on the tip interact much more strongly with the hydroxyl groups

at the surface than with the methyl groups leading to greater energy dissipation and hence a larger friction force. However, in order to test the ability of CFM to probe other types of interaction selectively, measurements were carried out on the same system using tips functionalized with a monolayer of dodecanethiol. These methyl terminated tips should probe selectively for the interfacial dispersion interactions. The results are also shown in Fig. 5. There is again a significant change in the adhesion force as the composition of the surface varies, but this time the adhesion force decreases as cosθ increases from 0 to 1. This seems to support the hypothesis that methyl terminated tips probe selectively for interfacial dispersion interactions, while polar tips probe selectively for polar interactions.

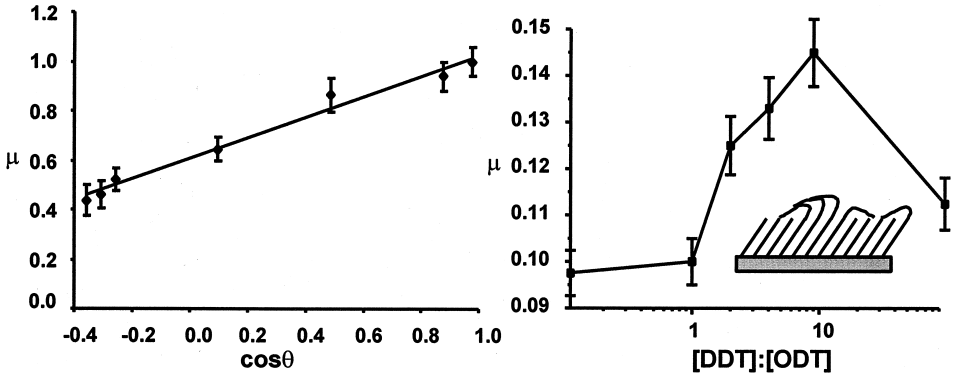

Fig. 6. Friction data for mixed SAMs. Left: variation of μ with cosθ (composition) for mixed monolayers formed from hydroxyl and methyl terminated SAMs. Right: variation of μ with the ratio of DDT (C_{12}) to ODT (C_{18}) in the solutions from which mixed SAMs containing these adsorbates were formed.

Friction forces were also measured for the same materials as a function of load, using carboxylic acid and methyl terminated tips. There have been a number of studies of the frictional properties of single component SAMs[26]. However, there have been, as yet, few studies of heterogeneous SAM systems[23,24,27]. The coefficient of friction, μ, was determined from the gradient of the friction-load plot for each material. Fig. 6 shows data for mixed SAMs composed of hydroxyl and methyl terminated adsorbates, measured using a carboxylic acid terminated tip. The variation in μ with cosθ is smooth, resembling the adhesion force data. For these materials, composed of adsorbates with identical alkyl chain lengths, it seems that the friction coefficients are correlated with the chemical compositions of the monolayers.

One of the possible consequences of plasma treatment of PET was the modification of surface mechanical properties through the fragmentation of polymer chains at the sample surface. In order to model the effect of changes in molecular organization on friction measurements by FFM, the friction behavior of monolayers composed of adsorbates with different alkyl chain lengths was also studied. Fig. 6 shows data for mixed SAMs formed by the coadsorption of octadecanethiol (ODT) and dodecanethiol (DDT). These adsorbates have identical terminal group chemistries, exhibit very similar surface free energies and exhibit very similar values of μ when formed into single component monolayers. However, when mixed monolayers of DDT and ODT are formed, the coefficient of friction changes markedly. The highest value measured is nearly 50% greater than that measured for either of the pure monolayers. Given the similarity in terminal group chemistry of these adsorbates, the explanation for this behavior must lie in terms of the molecular ordering.

Studies of this system by Laibinis *et al* have provided valuable insights into the SAM structures[28]. They have shown that a considerable excess of the shorter adsorbate in the solution from which the monolayer is formed is required in order for significant amounts of it to be present at the surface. Around the ratio of 9:1 DDT:ODT, the composition of the resulting monolayer is approximately 1:1 DDT:ODT, and for such monolayers, Laibinis *et al* have reported that infra-red spectroscopy reveals that significant numbers of *gauche* defects are present in the SAM. Their observations are consistent with a model for the structures of these SAMs in which longer adsorbates emerge from among shorter molecules, their alkyl chains collapsing on the surface to form a disordered outer layer, above an ordered inner film structure. This type of structure is illustrated rather loosely by the diagram included as an inset to the plot of μ vs composition. SAMs with other compositions exhibit declining numbers of *gauche* defects as either adsorbate comes to predominate in the monolayer. Accordingly one might expect the viscosity of the SAM surface to decline. This interpretation is consistent with the variations in the coefficient of friction presented in Fig. 6. The composition at which we measured the highest value of μ (9:1 DDT:ODT) corresponded approximately to that at which Laibinis *et al* measured the highest number of *gauche* defects. The viscous outer layer of these films is readily deformed, yielding a large contact area. The contact area is known to have a strong influence on the magnitude of the friction force in FFM[29], and a large friction coefficient might thus be expected for such materials. The declining values of μ either side of this composition reflect the decreasing numbers of *gauche* defects and reducing ease of deformation of the SAMs.

Friction and Adhesion: Plasma Treated PET

These studies of model heterogeneous systems provide a secure basis on which to attempt to understand the surface properties of plasma treated PET. In particular, we wished to examine the extent to which the incorporation of polar functional groups during treatment could be determined using SFM techniques. The effect of argon plasma treatment on the surface morphology of PET films has been extensively documented elsewhere[30,31]. In brief, the surface roughness changes very little, despite the fact that studies of the plasma treatment of Mylar D indicate that polymer erosion rates are as high as 4 nm min^{-1}. Studies of wettability indicated that the dispersion contribution to the surface free energy changes little, while the polar contribution increases markedly following plasma treatment. The principal effect on the surface chemical composition thus appears to be the incorporation of polar functionalities, a conclusion supported by XPS measurements. The work of adhesion was determined to increase rapidly, reaching a limiting value after 30 – 60 s.

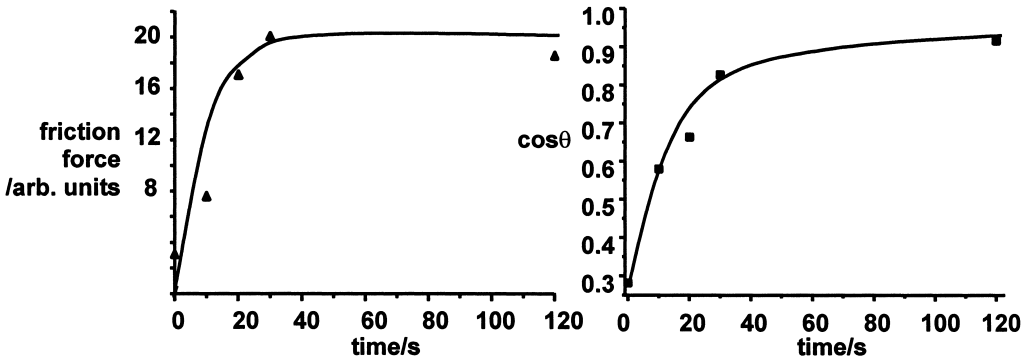

Fig. 7. Variation in the friction force (left) and the cosine of the water contact angle (right) for Melinex O following plasma treatment for varying times.

Initially, measurements of the friction force were made and compared with data from contact angle measurements (Fig. 7). It may be seen from these data that the friction force increases as the treatment time increases, with the rate of increase slowing significantly after 30 – 40 s. It therefore appears to follow the variation in cosθ quite closely, and it is tempting to ascribe the changes in the friction force to increases in the surface free energy. However, it was also known that imaging of the sample surface following plasma treatment of PET is problematic because of the comparatively easy deformation of the polymer surface following plasma treatment. In order to examine the relationship further, and test whether the variation in cosθ

did indeed explain the change in friction, a more detailed investigation was undertaken in which coefficients of friction and the adhesion forces were also measured.

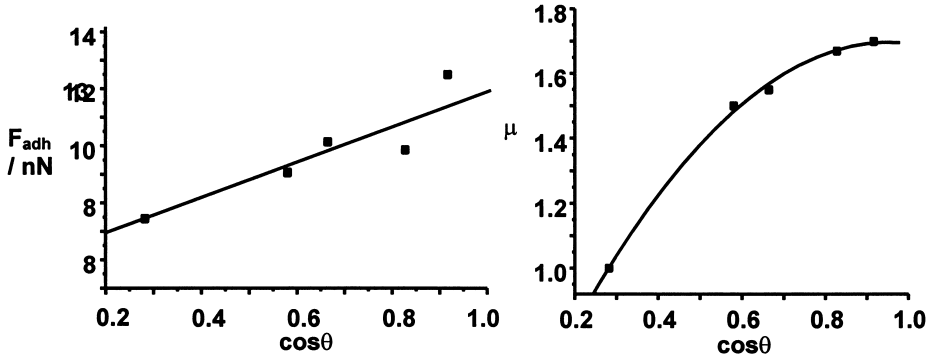

Fig. 8. Effect of plasma treatment on adhesion forces (left) and the coefficient of friction (right, normalized to untreated PET = 1.0) following exposure of Melinex O to an Ar plasma.

The increase in the adhesion force, measured with a polar tip, and the change in the friction coefficient (determined from friction-load plots and normalized to the value determined for untreated PET), are shown in Fig. 8 as a function of cosθ for argon plasma-treated samples of Melinex O. Cosθ is used again as a convenient measure of the extent of incorporation of polar groups at the surface following plasma treatment. The adhesion measurements reveal a steady increase with cosθ, to which a straight line may be fitted by linear regression. This mirrors the relationship between the adhesion force and cosθ measured for mixed methyl/hydroxyl and methyl/carboxylic acid terminated SAMs in both air and ethanol when polar tips were employed, suggesting that its magnitude is largely determined by the nature of the chemical interaction between the tip and the surface. In contrast, the relationship between μ and cosθ is clearly not linear. Repetition of the experiment a number of times reproduced the results very accurately and under no circumstances could a straight line be fitted by linear regression with a reasonable degree of confidence (by comparison, the data in Fig. 5 and for the mixed hydroxl/methyl terminated SAMs in Fig. 6 were fitted with a regression coefficient of 0.99). The data in Fig. 6 show that molecular organisation may have a profound influence on μ. It is believed that the non-linearity of the μ-cosθ plot results from the fact that plasma treatment causes a modification to the mechanical properties of the polymer surface, through chain scission, with the consequence that the tip-sample contact area increases (and hence the friction force[29]). Studies of Mylar D enabled an estimation of the rate of erosion of PET

during plasma treatment, by measuring the height difference between the tops of the silicate additives and the surrounding polymeric material[31]. It was found that the rate of erosion was substantial – of the order of 4 nm s^{-1}. It appears highly likely that the effect of the plasma is to cause rapid segmentation of polymer chains at the surface. The treated surface thus resembles a low molecular weight material. Undoubtedly, this would lead to more ready deformation of the tip during imaging in contact mode. This has been confirmed by studies using contact mode imaging with methyl terminated tips (to minimize tip-sample adhesion) and tapping mode[32]. Both these methodologies revealed a detailed morphology not observed in contact mode imaging. It was concluded that in contact mode, with a conventional silicon nitride tip, the surface is readily disrupted, resulting in a loss of detail in the image. This supports the picture of a mechanically weak outer layer following plasma treatment, and this could explain the non-linearity of the μ-cosθ plot: not only is the value of μ increased by the incorporation of polar groups at the surface, but it is increased also by the changed mechanical properties of the surface layer which result in an increased tip-sample contact area.

In contrast, the adhesion force measurements appear not to be influenced by the changed mechanical properties of the surface following plasma treatment. This is potentially very important for the characterization of complex, heterogeneous polymer surfaces. Our findings suggest that friction coefficient and adhesion force measurements are complementary. Analysis of both types of data together enables the determination of specific changes to the surface composition (*ie* the incorporation of polar or non-polar functionalities) and the separation of these chemical effects from changes to the order/mechanical properties of molecules at the surface. Moreover, the sensitivity of these techniques is more than adequate to probe rather subtle changes.

Conclusions

Using a suite of complementary techniques, including contact mode and tapping mode, friction force microscopy, phase imaging and chemical force microscopy, it has been possible to provide a detailed characterization of a complex polymer system and of the effects of plasma treatment on surface composition and properties. Novel insights have been provided into the polymer morphology. In particular, the present study reports some of the first images of crystallites in biaxially drawn PET films. A combination of chemical force microscopy and

friction force microscopy proved particularly effective in the characterization of plasma treated PET. Utilization of these complementary techniques enables the determination of both changes in the number of polar and non-polar groups at the polymer surface and changes in molecular order at the surface following plasma treatment.

Acknowledgements

The authors are grateful to Professor D Briggs (formerly ICI Wilton) for providing Melinex O with a detailed processing history, and for stimulating discussions, and to Dr R D Short (University of Sheffield) for providing details of the design of his plasma reactor. The authors thank EPSRC (grants GR/K88071 and GR/L78529) for financial support.

References

1. V. V. Tsukruk, *Rubber Chem. Technol.* **70**, 430 (1997).
2. S. N. Magonov and D. H. Reneker, *Annu. Rev. Mater. Sci.* **27**, 175 (1997).
3. P. Maivald, H. J. Butt, S. A. C. Gould, C. B. Prater, B. Drake, J. A. Gurley, V. B. Elings and P. K. Hansma, *Nanotechnol.* **2**, 103 (1991).
4. R. M. Overney, T. Bonner, E. Meyer, M. Ruetsche, R. Luthi, L. Howald, J. Frommer, H.-J. Guntherodt, M. Fujihara and H. Takano, *J. Vac. Sci. Technol. B* **12**, 1973 (1994).
5. R. M. Overney, E. Meyer, J. Frommer, D. Brodbeck, R. Luthi, L. Howald, H.-J. Guntherodt, M. Fujihara, H. Takano and Y. Gotoh, *Nature* **359**, 133 (1992).
6. C. M. Mate, *IBM J. Res. Develop.* **39**, 617 (1992).
7. C. D. Frisbie, A. Noy, L. F. Rozsnyai, M. S. Wrighton and C. M. Lieber, *Science* **265**, 2071 (1994).
8. C. D. Bain, E. B. Troughton, Y.-T. Tao, J. Evall, G. M. Whitesides and R. G. Nuzzo, *J. Am. Chem. Soc.* **111**, 321 (1989).
9. E. Cooper and G. J. Leggett, *Langmuir* **14**, 4795 (1998).
10. J. P. Cleveland, S. Manne, D.Bocek and P. K. Hansma, *Rev. Sci. Instrum.* **64**, 403 (1993).
11. D. F. Ogletree, R. W. Carpick and M. Salmeron, *Rev. Sci. Instrum.* **67**, 3298 (1996).
12. J. M. Neumeister and W. A. Ducker, *Rev. Sci. Instrum.* **65**, 2527 (1994).
13. J. Hazel and V. V. Tsukruk, *J. Tribol.*, **120**, 814 (1998).

14. A. W. Adamson, *Physical Chemistry of Surfaces*, 5th Edition, J. Wiley and Sons, New York, 1990, p. 460.
15. S. Lee, Y.-S. Shon, R. Colorado, R. L. Guenard, T. R. Lee and S. S. Perry, *Langmuir* **16**, 2220 (2000).
16. J. S. G. Ling and G. J. Leggett, *Polymer* **38**, 2617 (1997).
17. B. Sauer, R. S. McLean and R. R. Thomas, *Langmuir* **14**, 3045 (1998); A. Noy, C. H. Sanders, D. V. Vezenov, S. S. Wong and C. M. Lieber, *Langmuir* **14**, 1508 (1998); J. P. Pickering and G. J. Vancso, *Polym. Bull.* **40**, 549 (1998).
18. S. N. Magonov and D. H. Reneker, *Annu. Rev. Mater. Sci.* **27**, 175 (1997).
19. G. Bar, Y. Thomann, R. Brandsch, H.-J. Cantow and M.-H. Whangbo, *Langmuir* **13**, 3807 (1997).
20. J. B. Faisant de Champchesnel, D. I. Bower, I. M. Ward, J. F. Tassin, J. F. and G. Lorentz, *Polymer* **34**, 3763 (1993).
21. U. Goschel and G. Urban, *Polymer* **36**, 3633 (1995).
22. K. Feldman, T. Tervoort, P. Smith and N. D. Spencer, *Langmuir* **14**, 372 (1998).
23. B. D. Beake and G. J. Leggett, *Phys. Chem. Chem. Phys.* **1**, 3345 (1999).
24. H. I. Kim, M. Graupe, O. Oloba, T. Koini, S. Imaduddin, T. R. Lee and S. S. Perry, *Langmuir* **15**, 3179 (1999).
25. (a) S. R. Holmes-Farley, C. D. Bain and G. M. Whitesides, *Langmuir* **4**, 921 (1988); (b) C. D. Bain, J. Evall and G. M. Whitesides, *J. Am. Chem. Soc.* **111**, 7155 (1989).
26. Recent examples include:J. D. Kiely and J. E. Houston, *Langmuir* **15**, 4513; L. Li, Q. Yu and S. Jiang, *J. Phys. Chem. B* **103**, 8290 (1999); S. C. Clear and P. F. Nealey, *J. Coll. Interface Sci.* **213**, 238 (1999);A. R. Burns, J. E. Houston, R. W. Carpick and T. A. Michalske, *Langmuir* **15**, 2922 (1999); L. Qian, X. Xiao and S. Wen, *Langmuir* **16**, 662 (2000).
27. B. D. Beake and G. J. Leggett, *Langmuir* **16**, 735 (2000).
28. P. E. Laibinis, R. G. Nuzzo and G. M. Whitesides, *J. Chem. Phys.* **96**, 5097 (1992).
29. G. Bar, S. Rubin, A. N. Parikh, B. I. Swanson, T. A. Zawodzinski and M.-H. Whangbo, *Langmuir* **13**, 373 (1997).
30. B. D. Beake, J. S. G. Ling and G. J. Leggett, *J. Mater. Chem.* **8**, 1735 (1998).
31. B. D. Beake, J. S. G. Ling and G. J. Leggett, *J. Mater. Chem.* **8**, 2845 (1998).
32. B. D. Beake and G. J. Leggett, *Polymer* **40**, 5973 (1999).